ELSEVIER

Fire Safety Journal **29** (1997) 235–258

Printed in Northern Ireland
0379-7112/97/$17.00

PII: S0379-7112(97)00063-5

Strongly Buoyant Plume Similarity and 'Small-fire' Ventilation

G. G. Rooney* & P. F. Linden

Department of Applied Mathematics and Theoretical Physics, Silver Street, Cambridge CB3 9EW, UK

(Received 8 August 1996; revised version received 11 August 1997; accepted 10 September 1997)

ABSTRACT

We re-examine the problem of natural ventilation of a room containing a fire, in the light of recent results obtained by Rooney and Linden (1996) *concerning the similarity solution for non-Boussinesq plumes. We consider the case of a steady fire in a compartment with openings at floor and ceiling levels, and obtain expressions for the depth and density of the homogeneous ceiling layer maintained by the fire plume. Taking the limit of a large lower opening area, we compare our results with experiments performed by Thomas* et al. (1963). *We also perform a sample calculation to estimate the size of the difference between the weakly and strongly buoyant cases.* © 1998 *Elsevier Science Ltd.*

NOTATION

A	'Effective area' in Boussinesq ventilation model, see eqn (24)
$\tilde{A}$	'Effective area' in non-Boussinesq ventilation model, see eqn (28)
A_f	Area of floor covered by base of fire
a	Area of vent
B	Plume buoyancy flux
b	Plume radius
c_p	Specific heat capacity at constant pressure
D	Diameter of fire source
d	Upper-layer depth
F	Scaled density deficit, a conserved quantity with units of buoyancy flux, see eqn (15)
g	Gravitational acceleration
g'	Reduced gravity

* Author to whom correspondence should be addressed.

H Height of compartment ceiling
h Height of two-layer interface
K Upper-vent discharge coefficient (less than unity)
k Lower-vent pressure-loss coefficient (less than unity)
L Dimensionless constant in similarity solution, eqn (8)
l Flame length
M Dimensionless constant in similarity solution, eqn (9)
N Dimensionless constant in similarity solution, eqn (10)
p Length of perimeter of fire base
$\dot{Q}$ Convective power of fire
$\dot{Q}_t$ Total (convective and radiative) power of fire
r Radial distance from plume axis
T_0 Ambient temperature
V Plume volume flux
W Plume mass flux
w Vertical velocity
z Vertical distance above floor level
z_v Virtual-origin depth

Greek letters
α Plume entrainment constant
$\Delta\rho$ Plume/ambient density difference
Θ Ratio of upper-to-lower fluid densities, see eqn (26)
ξ Fractional interface height, see eqn (23)
ρ Density of plume
ρ_f Density of large-fire plume
ρ_0 Density of ambient (lower-layer) fluid
ρ_1 Density of upper-layer fluid

Subscripts
A Lower vent
B Interface
C Upper vent

1 INTRODUCTION

The toxic combustion products from accidental fires in modern buildings are a major hazard, and efficient removal of smoke from populated sections of a building is essential for safe evacuation in the event of such a fire. One means of smoke removal employed is natural (passive) ventilation, wherein smoke and fumes are vented to the atmosphere using the driving force of their own

buoyancy. For the venting of smoke from a building, 'displacement' ventilation is desired.

The essential point about displacement ventilation is that little or no mixing takes place between the contaminated air being removed and the fresh air which displaces it, and this is achieved through the thermal buoyancy of the contaminated air. This buoyancy, firstly, causes the contaminated air to collect in a layer in the upper part of a compartment (with fresh air below it forming a second layer) and, secondly, inhibits mixing by stabilizing the interface between the layers. Displacement ventilation therefore operates in a 'two-layer' system, with fresh air entering through vents lower than the interface, and contaminated air leaving from vents higher than the interface. It is clear that, in the absence of any other mechanism, the interface will move upward as the upper layer drains. (The vents should therefore be located as near to the floor and ceiling of the compartment as possible, so that displacement may occur for a range of interface heights.) If a fire continues to burn in the compartment, however, then the buoyant plume from the fire will pass through the interface and continually replenish the upper layer with combustion products. The entrainment of fresh air by the plume in the lower layer thus provides a means of mass transfer across the interface and, as entrainment causes the plume mass flux to increase with height, the height of the interface will determine the mass flux to the upper layer.

The absence of toxic fumes and blinding smoke from the lower layer makes it a useful clear passage for the evacuation of personnel, and facilitates the movement of fire fighters. The stable interface between the layers, which inhibits mixing between them, may be disrupted by fluid motions of sufficient kinetic energy to overcome the stabilizing influence of the buoyancy force. In this regard, it has been suggested[1] that natural ventilation may be better than forced ventilation, in which there is a danger that the displacing air may be pumped in at too great a rate, thus lowering the stability of the interface. If natural displacement ventilation is to be seriously considered as an option in building design for fire-safety, it is important to have a good quantitative understanding of its efficiency of operation. To contribute to this understanding, we here consider the application of a non-Boussinesq plume model to displacement natural ventilation, as a model of the ventilation behaviour of fires in buildings.

2 SMALL FIRES AS STRONGLY BUOYANT PLUMES

2.1 Large and small fires

We begin by briefly looking at the distinction between large and small fires.

In the work by Thomas *et al.*,[2] hereafter referred to as Paper I, a distinction is made between 'small fires' and 'large fires', depending solely upon the aspect ratio of the fire plume in the lower layer. More specifically, if the fire covers an area A_f of the floor, and the free plume extends to a height h above the floor before plunging through the interface, then Paper I states that small-fire theory applies for $A_f^{1/2}/h < 0{\cdot}5$, and large-fire theory applies for $A_f^{1/2}/h > 0{\cdot}5$.

2.1.1 *Large fires*

For large fires, Paper I gives the total mass flow W of entrained air into a fire of source perimeter p and density ρ_l, between the level of the source and height z as

$$W = 0{\cdot}096\, p\, \rho_0 \left(\frac{g\rho_l}{\rho_0}\right)^{1/2} z^{3/2} \tag{1}$$

based on assumptions about the mean vertical velocity and entrainment behaviour of large fires.

Following Paper I, the mass flux W in $\mathrm{kg\,s^{-1}}$ from a (large) fire is widely taken to depend on the source perimeter length p and the height above the source z, both in m, as

$$W = 0{\cdot}188\, p\, z^{3/2} \tag{2}$$

obtained from eqn (1) by substituting values for the fire and ambient densities, and for the gravitational acceleration g.[3]

Hinkley[4] presents comparison of the large-fire equation, eqn (2), with five sets of experimental results from four different experiments, with excellent agreement. Indeed, he reports the best line fit through the data considered as having the equation

$$W = 0{\cdot}189\, p\, z^{1{\cdot}5} \tag{3}$$

the data taken from fires having convective heat outputs per unit area in the range 34–1800 $\mathrm{kW\,m^{-2}}$, and perimeters in the range 0·7–16·2 m. This paper remarks upon the ease of application of the large-fire equation due to its independence of the strength of the fire and suggests that the limit of application of the large-fire equation be extended to cover fires in the range $A_f^{1/2}/h > 0{\cdot}1$.

Thomas[5] comments upon use of the large-fire equation that 'a theoretical justification is still awaited for this widely exploited extension of a simple flame correlation'.

In contrast to Hinkley's[4] excellent agreement, Dembsey *et al.*[6] compare data from experiments by nine different experimenters with a large-fire equation, obtained from the mass flux expression, eqn (1), by assuming values of the plume and ambient densities similar to those given by Drysdale.[3]

They find poor agreement between this model and the experiments considered, and suggest including a suitable virtual origin in the model as a means of correction. The suggested expression for the offset of the virtual origin depends on both the power of the fire and the source diameter, however.

2.1.2 *Small fires*

For small fires, Paper I quotes the plume volume flux from the plume similarity solution by Yih,[7] who gives the volume flux for the Boussinesq case as

$$V = 0{\cdot}153\left(\frac{Bz^5}{\rho}\right)^{1/3} \tag{4}$$

where

$$B\left(= -\int_0^\infty 2\pi r w g \Delta\rho \, dr \right) \tag{5}$$

is the (non-specific) buoyancy flux. In Paper I, the buoyancy flux in the Boussinesq case is related to the total (convective *and* radiative) power $\dot{Q}_t$ of the fire by

$$\frac{B}{\rho} = \frac{\dot{Q}_t g}{\rho_0 c_p T_0} \tag{6}$$

where the subscript 0 denotes ambient values, assumed constant. It is then conjectured that the non-Boussinesq volume flux may be obtained from the relationship given by Yih[7] by replacing the ambient density in eqn (6) by the plume density, although it is acknowledged that 'there is some uncertainty about the effect of significant departures' from the Boussinesq approximation. This replacement leads to an expression for the mass flux,

$$W = 0{\cdot}153\rho\left(\frac{g\dot{Q}_t}{c_p \rho T_0}\right)^{1/3} z^{5/3} \tag{7}$$

where the height z includes the depth of the virtual origin. This mass flux has the same dependences on height and buoyancy flux as a conventional Boussinesq plume model.[8]

2.1.3 *Near and far field*

More recently than Paper I, the data presented by McCaffrey[9] or Delichatsios[10] suggest that a fire begins to show plume-like (small fire) behaviour at the top of the flaming region, rather than at a fixed multiple of the base diameter. The flaming region is commonly termed the 'near field', and the region above this, the 'far field'. The flame length in buoyancy-dominated fires is a function of both the source diameter and the power output (see eqn (18)),

and so the height above which a fire may be deemed small would then depend on the burning rate and material as well as the geometry. This flaming region in buoyancy-dominated fires normally extends a few source diameters vertically.

In the near field, the fire may depart from the similarity behaviour predicted by the plume model for several reasons. For example, the diameter of the fire is non-negligible compared with the height of the near field and so introduces a new length scale into the problem, and in the combusting region the buoyancy flux is not a conserved quantity but increases with height. Attempts to model the flow above non-point sources in the near field using plume conservation equations[11] are unreliable because of uncertainty as to profile shape and entrainment behaviour in this region. More simply, the plume-similarity model is often applied close to the source using a 'virtual-origin' height correction, of the order of the source length scale, to compensate for disparities from the similarity form. The position of the virtual origin of a fire plume has been the subject of several previous studies (see, e.g. the summaries of Gupta[12] and Cox and Chitty[13]). The variety of correlations leads Gupta[12] to suggest that there is no single correlation which is applicable to all situations, and that the correlations available cannot be generalized. These observations together indicate that more work needs to be done to adequately understand the behaviour of fires in the near field.

2.2 Present model

It is shown by Rooney and Linden[14] that the similarity solutions for the mean vertical velocity w, radius b and reduced gravity g' of a non-Boussinesq plume are given by

$$w = LF^{1/3}z^{-1/3} \tag{8}$$

$$b = Mz\left(\frac{\rho}{\rho_0}\right)^{-1/2} \tag{9}$$

$$g' = NF^{2/3}z^{-5/3} \tag{10}$$

where z is the height above the (virtual) origin. F is a conserved quantity with the units of buoyancy flux (the dimensions of F are $[F] = L^4T^{-3}$), and L, M and N are constants related to each other and to the entrainment constant α by

$$N/L^2 = \tfrac{4}{3} \tag{11}$$

$$LM^2N = 1/\pi \tag{12}$$

$$M = 6\alpha/5 \tag{13}$$

so that

$$N^{-1} = \pi^{2/3} \tfrac{6}{5} \alpha (\tfrac{9}{10}\alpha)^{1/3} \tag{14}$$

This solution may be related to the far-field plume from a fire using the plume equations[14] to give

$$F = \frac{g\dot{Q}}{2c_p \rho_0 T_0} \tag{15}$$

where $\dot{Q}$ is the *convective* power of the fire.

The similarity solution, eqns (8)–(10), tends to the Boussinesq solution as $\rho/\rho_0 \to 1$, and from the expression of eqn (10) for the reduced gravity $g' = g\Delta\rho/\rho$ it is easily seen that this will occur when

$$z^{5/3} \gg \frac{N}{g} F^{2/3} \tag{16}$$

or, from eqns (14) and (15),

$$z \gg 0{\cdot}003 \left(\frac{\dot{Q}^2}{\alpha^4 g} \right)^{1/5} = 0{\cdot}01\, \dot{Q}^{2/5} \tag{17}$$

for height in m and $\dot{Q}$ in W, and taking typical values of the other parameters. Given that the flame length l in m has been correlated with the power output in W and the source diameter D in m by[3]

$$l \approx 0{\cdot}015 \dot{Q}_t^{2/5} - 1{\cdot}02D \tag{18}$$

we see that the fire plume may not be Boussinesq until a height of several flame lengths above the source.

The similarity solutions for reduced gravity and plume velocity in the strongly buoyant (non-Boussinesq) case are consistent with experimental observations for the centreline mean temperatures and velocities in strongly buoyant plumes outside the burning region, summarized by Delichatsios.[10] It is also interesting to note that the solution for the strongly buoyant plume radius agrees with Heskestad's[15] interpretation of Morton's[16] radial transformation.

The mass flux in the plume is then given by

$$W = \pi \rho b^2 w = N^{-1} \rho_0 \left(\frac{g\dot{Q}}{2c_p \rho_0 T_0} \right)^{1/3} z^{5/3} \tag{19}$$

Note that this expression is different in density dependence from the mass flux of eqn (7) conjectured in Paper I, but does, however, agree with the expression for the mass flux in Cetegen *et al.*,[17]

$$W = 0{\cdot}21 \rho_0 \left(\frac{g\dot{Q}_t}{c_p \rho_0 T_0} \right)^{1/3} z^{5/3} \tag{20}$$

2.3 Entrainment

Comparing the coefficients in eqns (7) and (20) with eqn (19), we find using eqn (14) that the numerical constant in eqn (7) corresponds to a value of the entrainment constant in the present model of $\alpha = 0{\cdot}124$, and the constant in eqn (20) (incorporating the estimated 25–30% difference between total and convective heat output) corresponds to a value of the entrainment constant of $\alpha = 0{\cdot}20$. Data for the Boussinesq case, as summarized by Turner,[18] suggest a value for the entrainment constant of $\alpha = 0{\cdot}083$. Thus, while the various values of α are all of the same order of magnitude, the non-Boussinesq/fire-plume entrainment constant is observed to be larger by a factor of approximately 2.

This discrepancy may be due to the experimental method of Cetegen *et al.*[17] They report, firstly, that fire-plume entrainment is subject to increase by ambient disturbances and, secondly, that their method of measuring plume mass flux is likely to overestimate because of the additional air entrained into the upper layer in the hood by disturbances at the interface, as the fire plume plunges through the interface into the upper layer. It is worth pointing out here that, in the measurements of entrainment by Ricou and Spalding,[19] the plume/jet was enclosed by a porous cylinder, with entrainment being estimated from the mass flux through the cylinder required to remove the pressure difference across it. These experiments led to an estimated value of $\alpha \approx 0{\cdot}08$ for jets, with a higher (unspecified) value for plumes, and, significantly, reduced entrainment for the case of combusting plumes/jets (mainly in the pre-mixed case). This experimental method would presumably lack most of the error associated with the hood method, the porous cylinder shielding the plume from ambient disturbances, and the absence of an upper layer discounting any possibility of excess entrainment.

3 NATURAL VENTILATION OF SMALL FIRES

3.1 Previous work

Relevant previous work in natural ventilation has been performed in Paper I, and by Linden *et al.*,[20] hereafter referred to as Paper II. Paper I considers the natural ventilation of a compartment above a small fire. The compartment consists of a horizontal ceiling containing a single vent, with a vertical screen around its perimeter extending downwards from ceiling level to some distance above the floor. The fire is at floor level, and the buoyant gases it produces rise and collect in the compartment, forming a hot layer. Figure 1 gives a schematic of this configuration. The hydrostatic pressure imbalance between the

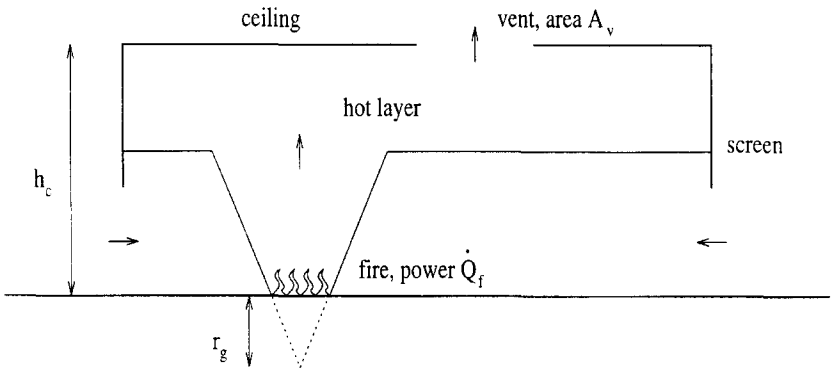

Fig. 1. Paper I experimental configuration.

inside and outside of the compartment, caused by the lower density of this layer, drives a flow through the compartment. After a short time this flow settles to a steady state, so that the depth of the hot layer becomes constant. Paper I considers both the case where the level of the hot layer is higher than the edge of the screen, so that all flow out of the compartment is through the vent and the flow between the screen and the floor is inward only, and the case where the level of the hot layer is lower than the edge of the screen, with fluid from the hot layer leaving the compartment below the screen as well as through the vent. In this second case, the flow between the screen and the floor is bidirectional, with hot gases leaving the compartment at the top of the gap, and ambient air flowing into the compartment lower down. Only the first case is relevant to our present study, so we will neglect those parts of Paper I which pertain to the second.

Data are presented from experiments performed on a rig as described above, with three settings of the vent area, and three settings of the screen depth. The fire is from a ring gas burner. The dimensions of the ceiling and the fire parameters are set out in Table 1. As stated previously, we are only concerned with the case where the hot layer is above the edge of the screen, and hence we omit the screen depth from our considerations.

The analysis in Paper I may be described as follows. A hydrostatic balance is performed on a box partially filled with buoyant fluid to obtain the hydrostatically driven mass flux through the opening. The interface height may then be predicted by matching this flux to the mass flux of a buoyant plume within the box (given by eqn (7)), which is the only mechanism of fluid transport across the buoyant/ambient interface.

The expression for the hot-layer depth d thus obtained (eqn (31) in Paper I),

$$Kad^{1/2} = 0{\cdot}043(z_v + H - d)^{5/2} \tag{21}$$

TABLE 1
Paper I Experimental Parameters

Symbol	*Quantity*	*Paper I value*	*S.I. equivalent*
h_c	Ceiling height	18 in	0·46 m
—	Ceiling length × width	24×36 in^2	$0{\cdot}61 \times 0{\cdot}91$ m^2
A_v	Vent areas	16, 24, 40 in^2	0·010, 0·016, 0·026 m^2
$\dot{Q}_f$	Heat output	2·1 Btu s^{-1}	2·2 kW
r_g	Depth of virtual origin	6 in	0·15 m

depends only upon the effective area of the top opening (Ka, where K is a constant less than unity), the room height H, and the depth z_v of the virtual origin of the fire. From consideration of the aspect ratio of a pure Boussinesq plume, it is stated that the depth of the virtual origin may be taken as a constant proportion of the horizontal dimension of the fire (i.e. the square root of the floor area covered by the fire). Therefore, based on this analysis, the depth of the hot layer is governed *only* by geometrical factors, and has no dependence on the power of the fire.

Paper I uses the plume mass flux in conjunction with the assumption that heat is conserved in the plume to obtain an expression for the temperature of the ceiling layer in terms of heat output, layer depth, ceiling height, and depth of the hot layer. It also states the form of the expression (similar to eqn (24)) to replace the vent area a in eqn (21) in the case where the screen becomes so low that the area of the gap between the screen and the floor also becomes one of the controlling factors in the system.

Paper II (and extensions thereof[21,22]) considers natural ventilation in the Boussinesq case, for a box of height H with small openings top and bottom such as that shown in Fig. 2. It contains analysis similar to that described above, using Bernoulli's theorem and the Boussinesq plume similarity solution to obtain an expression for the interface height h of

$$\left(\frac{\xi^5}{1-\xi}\right)^{1/2} N^{-3/2} = \frac{A}{H^2} \tag{22}$$

where

$$\xi = h/H \tag{23}$$

is the fractional height of the interface, and

$$A = \frac{K a_A a_C}{[\frac{1}{2}((K^2/k)\, a_C^2 + a_A^2)]^{1/2}} \tag{24}$$

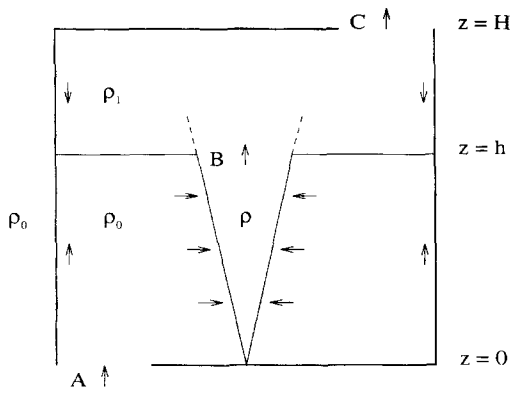

Fig. 2. Steady-state natural ventilation.

is the 'effective area', which is a function of the top and bottom opening areas, a_C and a_A. A also depends upon a pressure-loss coefficient k, which accounts for vent-edge effects on the inflow at A, and a discharge coefficient K which parameterizes the effect of the *vena contracta* at the outlet C. Expression of eqn (22) is used to examine the interface behaviour in the case of a single plume, multiple plumes, and plumes of different strengths. Vertically distributed sources of buoyancy within the box are also considered. The flow is again assumed to be steady, and fluid leaves the box by the top vent only. Comparisons are made with experiments recreating the above situations.

Notice that the interface position expression in Paper I, eqn (21), is the same as that in Paper II, eqn (22), for the limit of large lower-opening area, $a_A \to \infty$, if the interface height includes the depth of the virtual origin, and the upper-opening area includes a discharge flow-contraction coefficient.

3.2 Natural ventilation of a non-Boussinesq plume

We may use the model[14] of a non-Boussinesq fire plume to re-examine the problem of natural ventilation in the non-Boussinesq case. We refer to Fig. 2 for a schematic of the flow considered. This consists of a plume in a box of height H with openings at the top and the bottom. The plume within the box maintains a layer of fluid lighter than ambient (in the positively buoyant case) in the upper part of the box. Ambient fluid enters the box at A, is entrained by the plume, crosses the density interface as plume fluid at B, and leaves the box at C. The flow we consider is steady, so that the interface is at a fixed height $z = h$ above the floor. Using such a model means we tacitly assume that the fluid in the system is inhomogeneous in density and may change its density by

simple mixing, but by no other means, i.e. the fluid is incompressible everywhere except at the point of the plume source.

As detailed in the Appendix, we may show that the hot layer is homogeneous, and obtain expressions for the fractional height ξ of the interface, and the density ρ_1 of the upper layer,

$$\left(\frac{\xi^5}{1-\xi}\right)^{1/2} N^{-3/2} = \frac{\tilde{A}}{H^2} \tag{25}$$

and

$$\frac{\rho_1}{\rho_0} = \left(1 + \frac{N}{gH^{-5/3}} F^{2/3} \xi^{-5/3}\right)^{-1} \equiv \Theta(\xi) \tag{26}$$

where

$$\xi = h/H \tag{27}$$

and

$$\tilde{A} = \frac{\Theta^{1/2} K a_A a_C}{[\frac{1}{2}((K^2/k) a_C^2 + a_A^2/\Theta)]^{1/2}} \tag{28}$$

The relationship, eqn (25), represents the dependence of the fractional height of the interface upon the plume properties, the power of the fire and the geometry of the box. The plume properties are represented by N, which depends upon the entrainment constant α. The dependence upon the box geometry is contained in $\tilde{A}/H^2$. The non-Boussinesq nature of the flow, as represented by the power of the fire, is contained in Θ, the new term in this model compared with the Boussinesq case, eqns (22)–(24). Note that in the Boussinesq limit, $\Theta \to 1$, the power ceases to become a factor and $\tilde{A}/H^2$ is a purely geometrical term, representing the dependence of the interface height on the box height and the effective areas of the top and bottom openings. In this limit, the model is identical to that for one plume by Cooper and Linden.[21]

3.3 Comparison with Paper I

We now let $a_A \to \infty$ to compare the above model with the experiments in Paper I. In this limit we have that

$$\tilde{A} = \sqrt{2}\, K \Theta\, a_C \tag{29}$$

so that eqn (25) becomes

$$\left(\frac{\xi^5}{1-\xi}\right)^{1/2} N^{-3/2} = \sqrt{2}\, \Theta \frac{K a_C}{H^2} \tag{30}$$

TABLE 2
Cases Considered in Model Simulations

	H	
α	0·46 m	0·61 m
0·083	1	2
0·124	3	4
0·20	5	6

This equation is different from the expression in Paper I, eqn (21), in that it contains the term Θ which is a measure of the non-Boussinesq nature of the fire plume.

We may solve eqns (30) and (26) simultaneously for the various values of the entrainment constant α obtained from Paper I ($\alpha = 0{\cdot}124$), Cetegen *et al.*[17] ($\alpha = 0{\cdot}20$), and Turner[18] ($\alpha = 0{\cdot}083$), and the effective enclosure height, H, as either the actual enclosure height in Paper I ($H = 0{\cdot}46$ m), or the height used in Paper I as obtained from the enclosure height plus the depth of the virtual origin ($H = 0{\cdot}61$ m). We cannot estimate the virtual-origin depth from the expression given in Cetegen *et al.*[17] as the flame height of the fire in Paper I is not recorded. The cases we may therefore consider are listed in Table 2.

The best results for temperature vs. depth of the hot layer, and for hot-layer depth vs. upper-opening area, as compared with the experimental results of Paper I, are those for cases 2 and 3. These results are presented in Figs 3 and 4, together with the results of the Paper I small-fire theory outlined above. Case 2 shows good agreement with both temperature and depth for smaller ceiling-layer depths, whereas case 3 accurately predicts the upper-layer temperature, but underpredicts the layer depth. It may be seen from these figures that the Boussinesq model of Paper I gives results of similar accuracy to the non-Boussinesq model, and it is interesting to note from Fig. 4 that both the present model and the model of Paper I predict a continual increase of layer depth with vent area, whereas the data points seem to show a gradual levelling-off of layer depth, despite the increase in vent area. This interpretation of the data is somewhat uncertain as the size of the possible errors are unknown, however, it may indicate a more complicated behaviour at the vent than the simple flow contraction parameterized by K.

3.4 Parameter optimization

We may further consider optimizing the present model parameters to obtain the best fit to the Paper I data. The results of solving the present model with

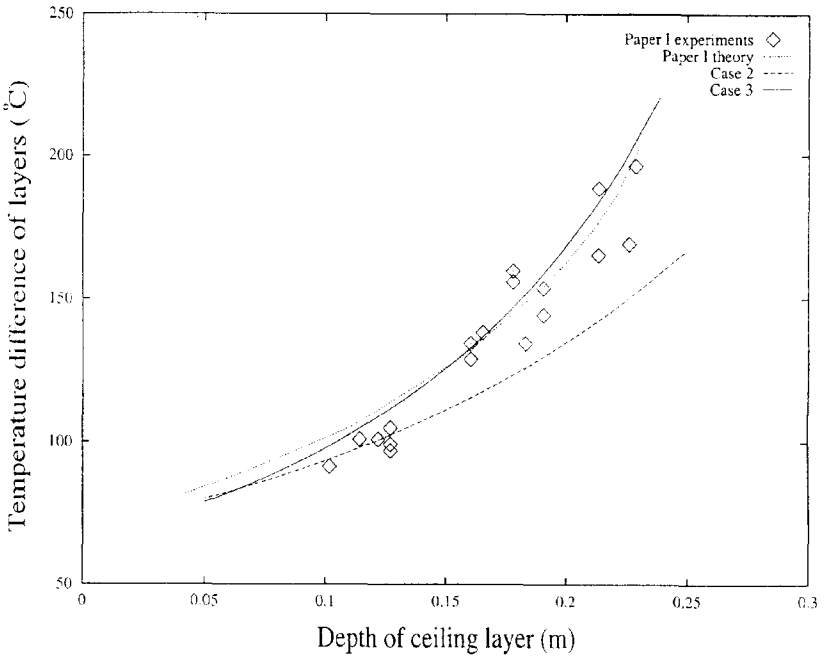

Fig. 3. Ceiling-layer temperature increase vs. depth.

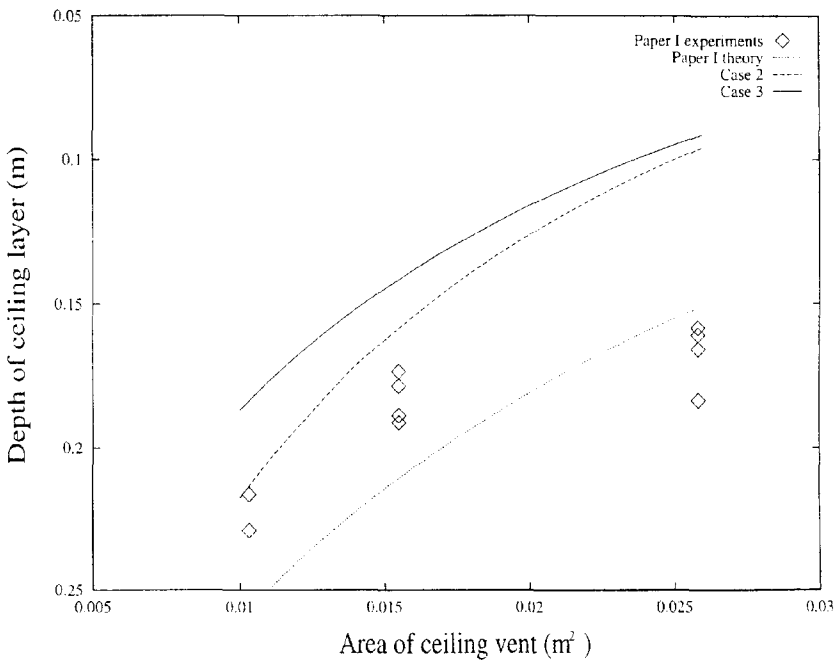

Fig. 4. Ceiling-layer depth vs. upper-opening area.

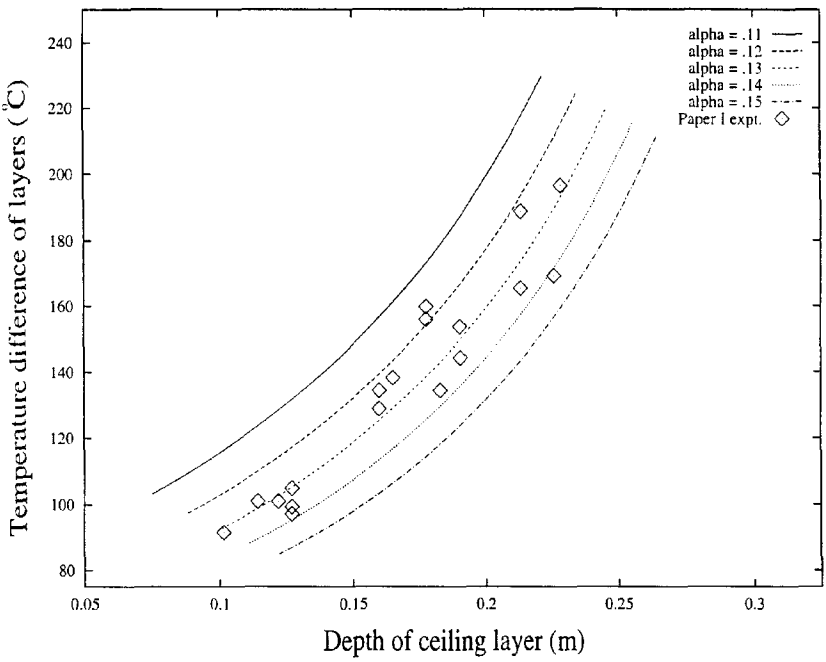

Fig. 5. Temperature vs. depth, varying α.

no virtual origin for varying values of the entrainment constant α are presented in Figs 5 and 6. It can be seen that attempting to optimize the fit with the other parameters at their present values will lead to a bad fit on both graphs. That is, the range of entrainment constant $0{\cdot}11 \leq \alpha \leq 0{\cdot}15$ contains the optimum fit to the data of temperature difference vs. layer depth, but only begins to touch on the data of layer depth vs. area. To two significant figures, the best fit on temperature difference (Figure 5) comes from a value of the entrainment constant of $\alpha = 0{\cdot}13$, with zero virtual origin.

A possible cause for the poor fit of the vent area vs. layer depth at this value of α may be the value of the discharge coefficient K. The value of $K = 0.6$ has been chosen in Papers I and II as representing the value for a laminar *vena contracta*, but it is likely that additional turbulent dissipation at the outlet in the Paper I experiments imply a lower value than this. We may therefore hold the entrainment constant at the optimum value (for the temperature data) of $\alpha = 0{\cdot}13$ and seek to obtain a better fit to the vent-area data by varying K. Clearly, additional dissipation will lead to a smaller outflow through the vent, and so we should consider values of K less than 0·6. A lower value of K will reduce the *effective* upper-vent area Ka_C, which should therefore lead to a greater layer depth (lower interface) for the same *actual* vent area a_C.

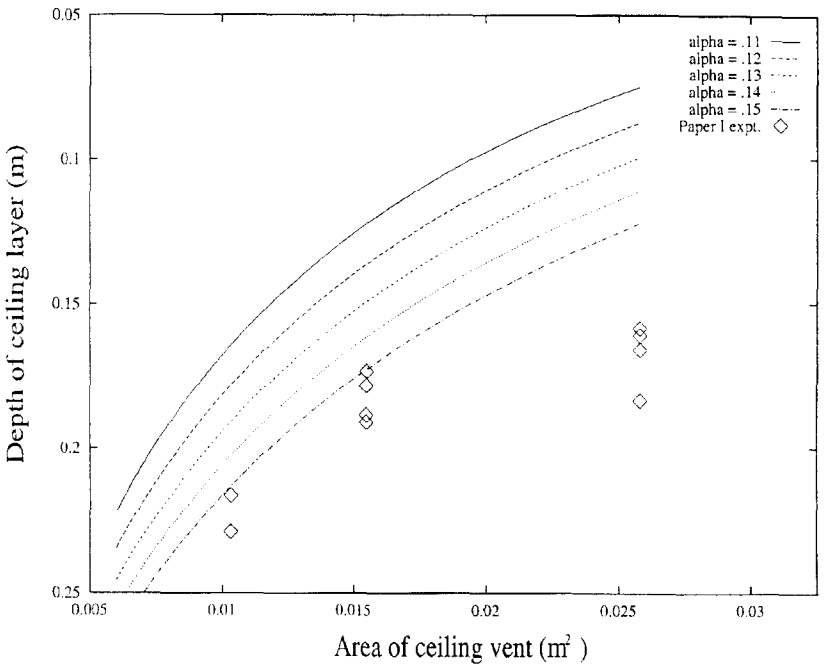

Fig. 6. Depth vs. area, vaying α.

The curve for $\alpha = 0{\cdot}13$ on Fig. 6 shows that an increase in depth is indeed required to produce a better fit. We find that, to one significant figure, the optimum value of the discharge coefficient is found to be $K = 0.4$, and the results of the simulation with these values ($\alpha = 0{\cdot}13$, $K = 0{\cdot}4$, no virtual origin) are presented in Figs 7 and 8.

When considering optimization w.r.t. the vent-area data, greater emphasis has been placed on the data points for the two lower vent-area values. This is because, between the middle and largest-area sets of points, the value of the vent area has increased by more than half without the measured layer depth changing by any great amount. This is possibly due to the actual flow departing from our ideal picture as the layer depth decreases and the vent area increases, e.g. by the momentum with which the plume enters the upper layer having some effect on the upper-layer flow. We therefore expect the datapoints at lower vent areas to better represent the flow in the present model.

3.5 Comparison with Boussinesq ventilation

We may now make a sample comparison of our model with its Boussinesq limit, in order to obtain an estimate for the magnitude of non-Boussinesq

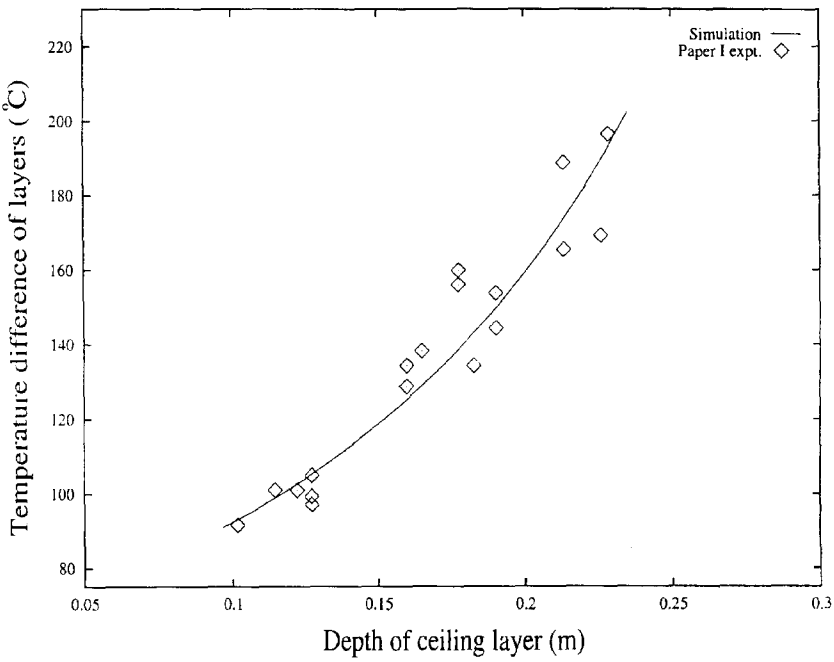

Fig. 7. Temperature vs. depth, optimum values.

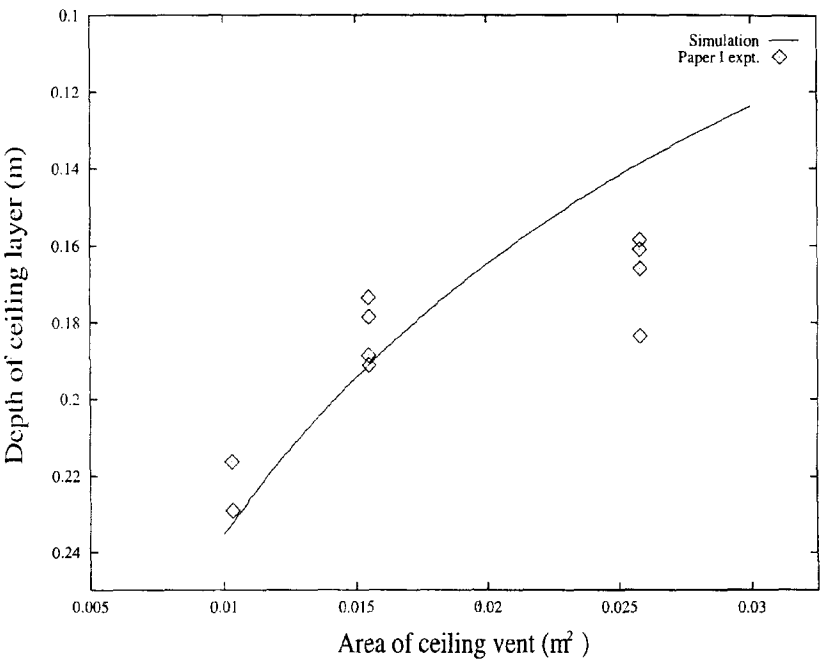

Fig. 8. Depth vs. area, optimum values.

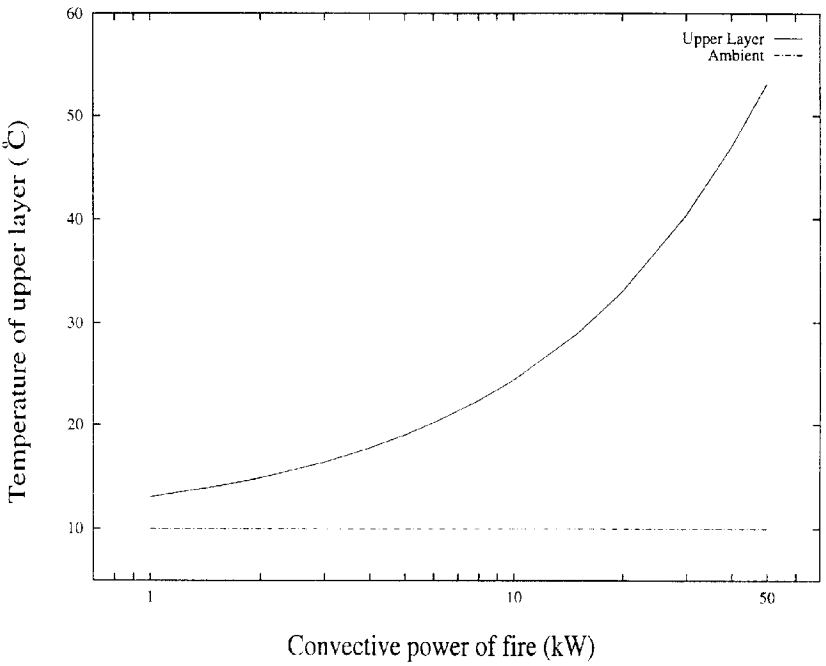

Fig. 9. Temperature of upper layer vs. convective power of the fire, case 3 values.

effects in a particular natural ventilation problem. We will firstly use the parameters from case 3 above, i.e., we will take the entrainment constant to have a value of $\alpha = 0{\cdot}124$, and omit virtual-origin corrections. We take this to be the best case for the parameter values obtained by previous workers.

Our sample comparison is performed for a compartment 2·5 m high, with openings top and bottom each of area 1·0 m^2, and for fires in the range 1–50 kW, a range in which fires may still be thought of as 'small' for this size of enclosure. (While a small fire is so-called solely on account of its geometrical dimensions, the empirical correlation between flame length, source diameter, and power, eqn (18), indicates that the above range is representative of a small fire in the size of enclosure considered.) The results are presented in Figs 9 and 10. The ambient temperature has been specified as 10°C, and so this is added in the temperature plot, Fig. 9. We see that the layer depth does increase, but fractionally by very little, approximately 5 cm difference in a 2.5 m enclosure.

We may carry out the same simulation using the parameter values of $\alpha = 0{\cdot}13$, $K = 0.4$ obtained by optimizing the model. The results for this case are presented in Figs 11 and 12. Again, we see that the layer depth, while lower than in the other case, is little affected by departures from the Boussinesq value.

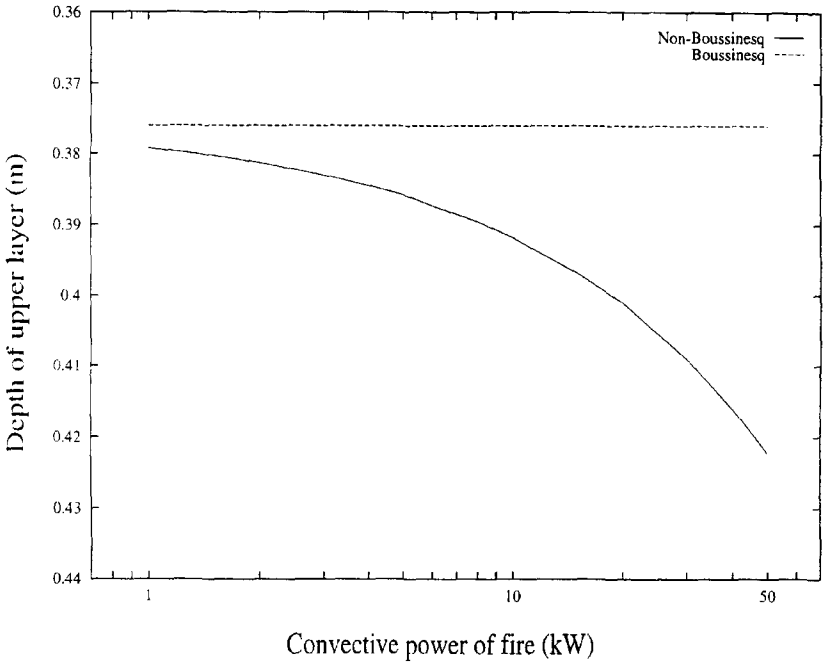

Fig. 10. Depth of upper layer vs. convective power of the fire, case 3 values.

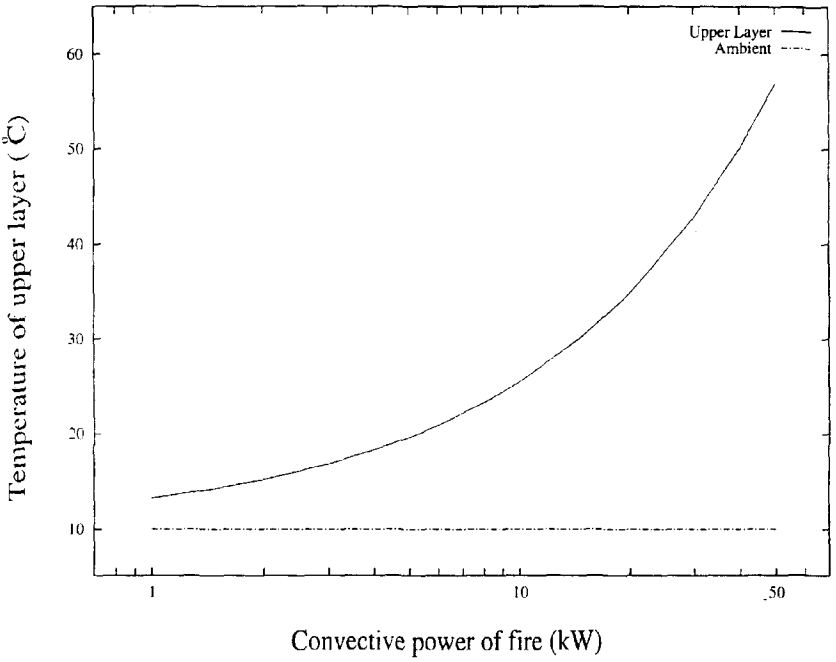

Fig. 11. Temperature of upper layer vs. convective power of the fire, optimized values.

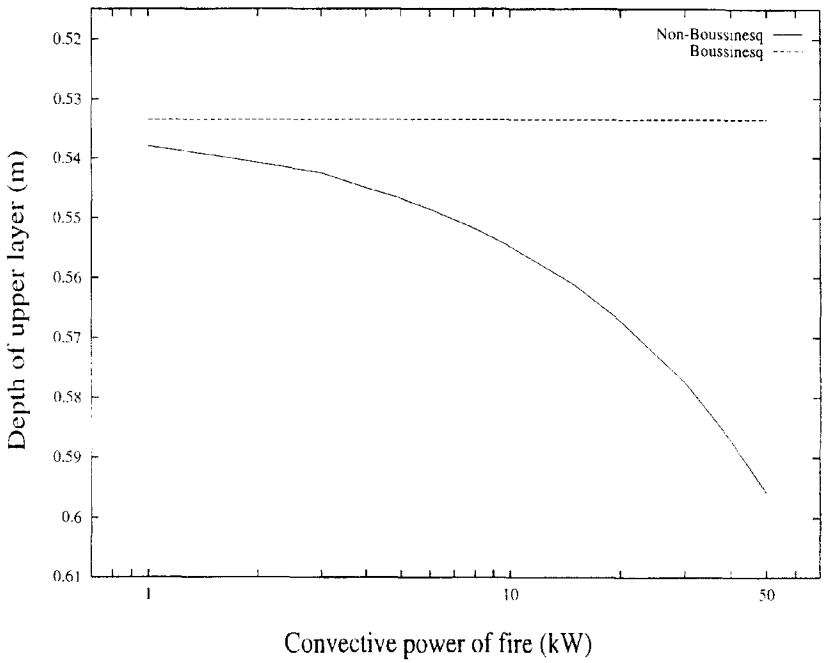

Fig. 12. Depth of upper layer vs. convective power of the fire, optimized values.

Therefore, with either set of parameters in this case, the method in Papers I and II of calculating the upper-layer temperature from conservation of heat flux or reduced gravity, and calculating the layer depth from the Boussinesq interface expression, ought to give reasonably accurate results.

4 CONCLUSIONS

We have considered the natural ventilation of fires in enclosures, using the non-Boussinesq plume theory developed elsewhere. This is an important concern, as previous models of natural ventilation have incorporated non-Boussinesq corrections either incorrectly (based on conjecture), or not at all. We have therefore applied our present model to the problem, and compared it with experimental data from Thomas *et al.*[2] From this comparison, the most appropriate value of the entrainment constant has been selected, and used in the simulation of a model problem of small fires in a room-sized, ventilated compartment. We have also optimized the entrainment constant and the output discharge coefficient to obtain a best fit to these data, and used these values to simulate the model problem.

Optimizing the entrainment constant, rather than using the most accurate laboratory measurement, is permissible given the observations of Cetegen *et al.*[17] and others that small ambient disturbances can greatly increase the mass flux in a plume. As it is unlikely that an accidental fire in a ventilated building will proceed in a completely quiescent ambient, the best procedure when making predictions of ventilation behaviour is probably to ensure that model estimates of ceiling-layer temperature and depth are accompanied by clearly stated likely errors arising from the possible range of variation of α. Secondly, it can be seen from Figs 9–12 that varying the discharge coefficient K results in a similar fractional change in the layer depth ($\approx 40\%$), but a much smaller change in temperature, as the layer-depth change is still small compared to the plume length. Opimizing K (or even possibly introducing a function depending on outlet area and/or velocity, say) will undoubtedly lead to a more accurate model.

Finally, although we have shown that the non-Boussinesq region of a fire plume may extend several flame lengths into the far field, the model simulation indicates that the non-Boussinesq departures from Boussinesq ventilation values are small, and so Boussinesq theory can be applied with reasonable confidence when simulating the natural ventilation of small fires. As stated previously, the term 'small fire' refers solely to the geometry of the fire plume, and imparts no information about the power output of the fire. However, for a fire with a convective power output such that non-Boussinesq effects would significantly alter the ventilation behaviour, it seems that the likely geometrical size of such a fire would render a 'small-fire' model of the type used here inappropriate.

ACKNOWLEDGEMENTS

This work was supported by a research studentship from the Department of Education for Northern Ireland, and by a CASE studentship from the Health & Safety Executive.

REFERENCES

1. Kramer, C. & Gerhardt, H. J., Ventilation and heat smoke extraction from industrial buildings. *J. Wind Engng Ind. Aerodyn.*, **29** (1988) 309–35.
2. Thomas, P. H., Hinkley, P. L., Theobald, C. R. & Simms, D. L., Investigations into the flow of hot gases in roof venting. *Fire Research Technical Paper No.* 7, Fire Research Station, Watford, UK, 1963.
3. Drysdale, D., *An Introduction to Fire Dynamics.* Wiley, New York, USA, 1985.
4. Hinkley, P. L., Rates of 'production' of hot gases in roof venting experiments. *Fire Safety J.*, **10** (1986) 57–65.

5. Thomas, P. H., On formulae for the movement of smoke in fires. *Fire Sci. Tech.*, **9**, (1989) 1–3
6. Dembsey, N. A., Pagni, P. J. & Williamson, R. B., Compartment fire near-field measurements. *Fire Safety J.*, **24** (1995) 383–419.
7. Yih, C. S., Free convection due to a point source of heat. In *Proc. 1st US Nat. Congr. Appl. Mech.*, 1952, pp. 941–7.
8. Morton, B. R., Taylor, G. I. & Turner, J. S., Turbulent gravitational convection from maintained and instantaneous sources. *Proc. Roy. Soc.*, **A234** (1956) 1–23.
9. McCaffrey, B. J., Purely buoyant diffusion flames: some experimental results, National Bureau of Standards, NSBIR 79-1910, 1979.
10. Delichatsios, M. A., On the similarity of velocity and temperature profiles in strong (variable density) turbulent buoyant plumes. *Combust. Sci. Technol.*, **60** (1988) 253–66.
11. Gupta, A. K., Kumar, S. & Singh, B., Plume analysis above finite-size fire sources In *Fire Safety Science, Proc. 3rd Int. Symp.*, 1991, pp. 445–54.
12. Gupta, A. K., Fire-plume theories and their analysis. *J. Appl. Fire Sci.* **2** (1993) 269–98.
13. Cox, G. & Chitty, R., Some source-dependent effects of unbounded fires *Combust. Flame*, **60** (1985) 219–32.
14. Rooney, G. G. & Linden, P. F., Similarity considerations for non-Bossinesq plumes in an unstratified environment. *J. Fluid Mech.*, **318** (1996) 237–50.
15. Heskestad, G., Fire plume air entrainment according to two competing assumptions. *Proc. 21st Int. Symp. on Combustion*, 1986, pp. 111–20.
16. Morton, B. R., Modelling fire plumes. *Proc. 10th Int. Symp. on Combustion*, 1965, pp. 973–82.
17. Cetegen, B. M., Zukoski, E. E. & Kubota, T., Entrainment in the near and far field of fire plumes. *Combust. Sci. Technol.* **39** (1984) 305–31.
18. Turner, J. S., Turbulent entrainment: the development of the entrainment assumption, and its application to geophysical flows. *J. Fluid Mech.*, **173** (1986) 431–71.
19. Ricou, F. P. & Spalding, D. B., Measurements of entrainment by axisymmetrical turbulent jets. *J. Fluid Mech.*, **8** (1961) 21–32.
20. Linden, P. F., Lane-Serff, G. F. & Smeed, D. A., Emptying filling boxes : the fluid mechanics of natural ventilation. *J. Fluid Mech.*, **212** (1990) 303–14.
21. Cooper, P. & Linden, P. F., Natural ventilation of an enclosure containing two buoyancy sources. *J. Fluid Mech.*, **311** (1996) 153–76.
22. Linden, P. F. & Cooper, P., Multiple sources of buoyancy in a naturally ventilated enclosure. *J. Fluid Mech.*, **311** (1996) 177–92.

APPENDIX

We refer to Fig. 2 for the positions A, B, C etc. in the ventilation system.

For the steady-state case with the presence of a plume, we must replace the conservation of vertical volume flux with the conservation of vertical mass flux, i.e. the vertical mass flux W through any horizontal plane must be constant, and in particular,

$$W_A = W_B = W_C \tag{A1}$$

We note the difference that the presence of the plume makes. It provides a mechanism for transferring fluid from the lower layer to the upper whilst keeping the interface steady. Without the plume, the interface would have to move, and we would be forced to have conservation of volume flux. We may interpret the change to the conservation of mass flux in, e.g. the case of thermal buoyancy as showing that the ambient air is heated at the plume source and expands by a significant amount, so that a greater volume flux is needed at the exit to maintain the steady state.

Paper II uses the conservation of buoyancy flux between B and C to demonstrate that the density of the upper layer is uniform. We may obtain the same result here, either from the conservation of buoyancy flux or the conservation of 'pseudo-buoyancy flux' F,

$$F_B = F_C,\ W_B = W_C \Rightarrow \rho_B = \rho_C$$
$$\Rightarrow \rho|_{h \le z \le H} = \rho_1, \text{ const} \tag{A2}$$

i.e. the upper layer is of uniform density ρ_1 equal to the plume density at B.

We may also use Bernoulli's theorem to obtain a relationship between the entry and exit velocities and the hydrostatic head,

$$w_C^2 = 2g'(H - h) - \frac{w_A^2}{k}\frac{\rho_0}{\rho_1} \tag{A3}$$

where $k(<1)$ is a pressure loss coefficient to account for vent-edge effects upon the inflow at A. This is almost identical to the Boussinesq case, except for the factor of ρ_0/ρ_1 on the r.h.s., which would be unity in that case.

If we denote the area of an opening by a, we have from eqn (A1) that

$$w_C^2 = w_A^2\left(\frac{a_A\rho_0}{Ka_C\rho_1}\right)^2 \tag{A4}$$

where K is a discharge coefficient, as used in Paper I and by Cooper and Linden.[21] Combining this mass balance with eqn (A3) gives

$$w_A^2 = \frac{2g'(H - h)}{(1/k)(\rho_0/\rho_1) + (a_A\rho_0/Ka_C\rho_1)^2} \tag{A5}$$

We may now obtain the interface height from the plume similarity solution, eqns (8)–(10) by matching the mass flux in the plume at B with the mass flux at A obtained from the velocity at A.

Rearranging eqn (10) gives the expression for the ratio of plume to ambient densities,

$$\frac{\rho}{\rho_0} = \frac{1}{1 + (NF^{2/3}/g)\,z^{-5/3}} \tag{A6}$$

and so the ratio of the densities in the upper and lower layers is given by

$$\frac{\rho_1}{\rho_0} = \frac{\rho}{\rho_0}\bigg|_{z=h} = \frac{1}{1 + (NF^{2/3}/g)h^{-5/3}} = \Theta(h), \text{ say} \tag{A7}$$

This is equivalent to obtaining the upper-layer temperature from conservation of heat flux in the plume, which is the method used in Paper I, or to obtaining the reduced gravity of the upper layer from the reduced gravity of the plume, as in Paper II.

We may also obtain the mass flux at B, which is given by

$$W_B = \pi w b^2 \rho|_{z=h} = N^{-1}\rho_0 F^{1/3} h^{5/3} \tag{A8}$$

Hence, from eqns (A1), (10), and using

$$W_A^2 = \rho_0^2 w_A^2 a_A^2 \tag{A9}$$

eqn (A5) becomes the expression for the interface height,

$$\left(\frac{\xi^5}{1-\xi}\right)^{1/2} N^{-3/2} = \frac{\tilde{A}}{H^2} \tag{A10}$$

where

$$\xi = h/H \tag{A11}$$

is the fractional height of the interface, and

$$\tilde{A} = \frac{\Theta^{1/2} K a_A a_C}{[\frac{1}{2}((K^2/k)a_C^2 + (a_A^2/\Theta))]^{1/2}} \tag{A12}$$